ISSN (Print) 1226-1750
ISSN (Online) 2233-6656
**Journal of Magnetics** 18(3), 276-282 (2013) http://dx.doi.org/10.4283/JMAG.2013.18.3.276

# Analysis and Case Study of Permanent Magnet Arrays for Eddy Current Brake Systems with a New Performance Index

**Surenkhorloo Sainjargal and Jin-Kyu Byun***

*School of Electrical Engineering, Soongsil University, Seoul 156-743, Korea*

(Received 7 May 2013, Received in final form 29 May 2013, Accepted 1 June 2013)

**In this paper, magnetic flux distributions of several permanent magnet arrays, including Halbach array, are analyzed and compared. Also, braking force characteristics on a moving solid conductor in the eddy current brake systems with such magnet arrays are analyzed. Then, a new performance index taking into account the maximum braking force and the volume of the magnet is introduced for the comparison and case study of permanent magnet arrays. By changing the lengths, magnetization directions and the height of the permanent magnet arrays, a higher braking force per volume of the magnet can be achieved.**

**Keywords :** eddy current brake, halbach array, performance index, permanent magnet

## 1. Introduction

Traditional friction brakes are composed of two functional parts: a rotor connected to the wheels and a stator fixed to the chassis of the vehicle. These brakes pose several problems, especially in hybrid vehicles: significant wearing, fading, complex and slow actuation, lack of fail-safe features, increased fuel consumptions due to power assistance, and requirement for anti-lock controls. To solve these problems, eddy current brakes have been developed.

The eddy current brake exhibits less wear and noise compared to the traditional mechanical friction brake, and it has excellent braking performances at high speed. However, there are disadvantages, such as the strong heat and thermal metamorphism due to the generation of the induced currents, and very weak braking force at low speeds. Nevertheless, because of the advantages of non-contact brake that are effective at high speeds with short response times, it is widely used in many controlled braking applications [1-3].

In the design of eddy current brakes with permanent magnet (PM) arrays, one of the easy solutions to improve the braking force characteristics is to increase the volume of the magnets. However, the total volume of the magnet is also one of the deciding factors for the total cost of the system. For this reason, in many of the previous works on eddy current brake design, the volume of the magnet was set to be constant [4-7]. However, such constant magnet volume condition may prevent the cost-efficient PM array design. In this paper, we propose a new performance index considering maximum braking force and total magnet volume. We analyze and compare several different PM array structures according to this performance index. We also change magnetization direction, magnet length, and magnet height, and analyze their influences on the braking force itself and the performance index.

## 2. Governing Equations for Eddy Current Brake

An eddy-current brake consists of a stationary source of magnetic flux (permanent magnet or electromagnet) in front of a moving conductor (metal disc, drum or fin). Because of the motion, the conductor experiences a time-varying magnetic flux density, which according to Faraday's law, induces electric field in the conductor. This electric field results in circulating eddy-currents in the conductor by Ohm's law. The interaction of eddy-currents with the flux density results in a force that opposes the motion. When the magnetic poles are excited by the permanent magnet, the current source is zero. With zero current source condition, the governing equation for the electromagnetic field problem with eddy currents due to

©The Korean Magnetics Society. All rights reserved.
*Corresponding author: Tel: +82-2-820-0644
Fax: +82-2-817-7961, e-mail: jkbyun@ssu.ac.kr

© 2013 Journal of Magnetics

motion is:

$$\nabla \times \mathbf{H} = \mathbf{J_e} \tag{1}$$

with

$$\mathbf{E} = \boldsymbol{v} \times \mathbf{B} \tag{2}$$

where $\mathbf{J_e}$ is eddy current density induced in the rail, and $\boldsymbol{v}$ is relative velocity of the conductor. In the presence of a permanent magnet, the quantities $\mathbf{B}$ and $\mathbf{H}$ are related through the remanent flux density $\mathbf{B}_r$ of the magnet as:

$$\mathbf{B} = \mu_0 \mu_r \mathbf{H} + \mathbf{B}_r \tag{3}$$

where $\mu_r$ is relative permeability. The eddy current due to motion is given by,

$$\mathbf{J}_e = \sigma \mathbf{E} = \sigma(\boldsymbol{v} \times \mathbf{B}) \tag{4}$$

where $\sigma$ is the conductivity of moving secondary side. Using (3) and (4), (1) can be written as,

$$\nabla \times \left\{ \frac{1}{\mu_0} \frac{1}{\mu_r} (\nabla \times \mathbf{A} - \mathbf{B}_r) \right\} = \sigma \boldsymbol{v} \times (\nabla \times \mathbf{A}) \tag{5}$$

where $\nabla \times \mathbf{A} = \mathbf{B}$ and $\mathbf{A}$ is the magnetic vector potential. Assuming the motion is only in the $x$-direction and the eddy current only has $z$-component, the $\boldsymbol{v} \times (\nabla \times \mathbf{A})$ term in (5) becomes,

$$\boldsymbol{v} \times (\nabla \times \mathbf{A}) = v_x \left( -\frac{\partial A_z}{\partial x} \right) \mathbf{a}_z . \tag{6}$$

Consequently, the governing equation for the 2-dimensional analysis of PM eddy current brake can be expressed as:

$$-\frac{1}{\mu_0 \mu_r} \left( \frac{\partial^2 A_z}{\partial x^2} + \frac{\partial^2 A_z}{\partial y^2} \right) + \sigma v_x \frac{\partial A_z}{\partial x} = \frac{1}{\mu_0 \mu_r} \left( \frac{\partial B_{r_y}}{\partial x} - \frac{\partial B_{r_x}}{\partial y} \right), \tag{7}$$

where Galerkin's method can be applied for the finite element formulation.

## 3. Analysis and Comparison of Permanent Magnet Arrays

The eddy current brake systems considered in this paper are composed of permanent magnet arrays and secondary conductor fins. In this chapter, the permanent magnet arrays with different magnetization patterns and iron core structures are analyzed, and their magnetic field distributions and braking force characteristics are compared. All these topologies are developed for the single-sided structure, where the secondary is a nonmagnetic conducting fin (aluminum). Table 1 shows the structural dimensions and the material properties of the eddy current brake system.

**Table 1.** Dimensions and material properties for the eddy current brake system.

| | Parameters | Value |
|---|---|---|
| Permanent Magnet (1 block) | dimensions [mm] | 25 × 25 × 50 |
| | remanent flux density, $B_r$ [T] | 1.14 |
| Iron Core (1 block) | dimensions [mm] | 25 × 25 × 50 |
| | relative permeability, $\mu_r$ | 4,000 |
| Conducting Fin (aluminum) | dimensions [mm] | 275 × 10 × 50 |
| | electric conductivity, σ [S/m] | $3.45 \times 10^7$ |
| Air gap | size [mm] | 5 |

The magnetic field distributions and braking forces on the moving conductor are calculated and analyzed using the COMSOL Multiphysics software [8] based on finite-element formulation given in Chapter 2. The braking force is calculated by integrating Maxwell stress tensor around the conductor boundary [9].

Fig. 1 shows three PM arrays we analyzed in this chapter. Array a is a Halbach array, and array b is composed of horizontally-magnetized magnets separated by iron cores. Finally, the array c is composed of vertically-magnetized magnets separated by iron cores.

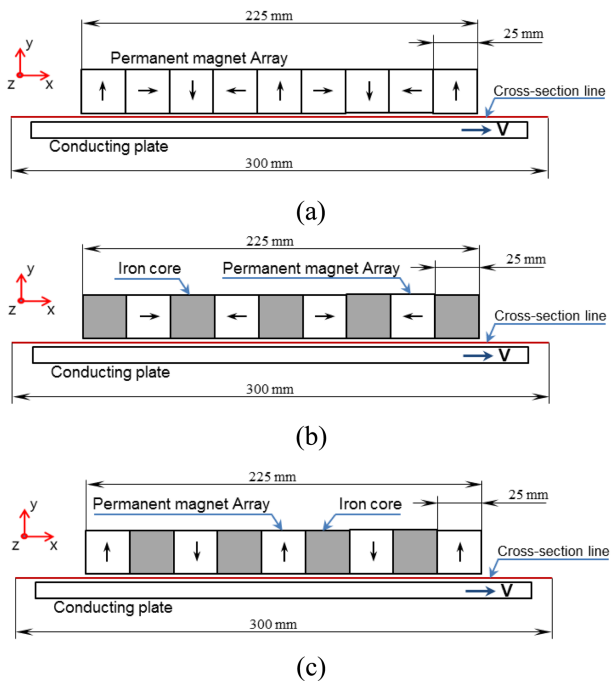


**Fig. 1.** (Color online) Permanent magnet arrays for linear eddy-current brake systems. (a) Array ⓐ (Halbach array). (b) Array ⓑ (horizontally-magnetized magnets separated by iron cores). (c) Array ⓒ (vertically-magnetized magnets separated by iron cores).

### 3.1. Magnetic flux density and braking force comparison

The static magnetic field distributions of different PM arrays without conductor secondaries are shown in Fig. 2(a), 3(a) and 4(a), respectively. The flux distributions of PM arrays with iron cores are symmetrical with respect to a horizontal line that goes through the center of the PM arrays (Fig. 3(a) and 4(a)), and it can be seen that the flux of PM array with iron cores will turn toward a metal frame (which is not shown in the figures) of the eddy current brake when the conductor is not present. Thus, it is necessary to shield magnetic flux for these iron-core PM arrays using primary back-iron as the magnetic flux path. Meanwhile, in the Halbach array, when the conductor is not present, the lower side has much stronger flux density compared to the upper side of the array (Fig. 2(a)), and the field distribution is asymmetrical. This shows that Halbach magnetized topology has an inherent self-shielding property and, therefore, does not require the primary back-iron for the magnetic flux path [10].

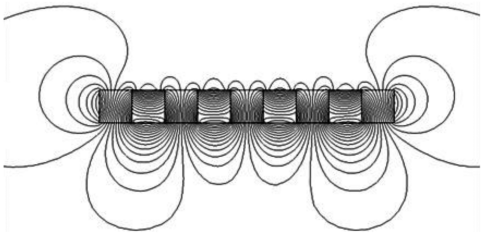

(a)

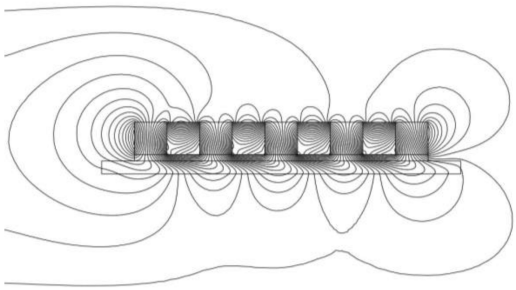

(b)

**Fig. 2.** Magnetic flux distributions of a Halbach array ⓐ. (a) No conductor. (b) With moving conductor ($v$ = 10 m/s).

The flux distributions of each model when the conductor secondary is moving with constant velocity of $v$ = 10 m/s with 5 mm air-gap is shown in Fig. 2(b), 3(b) and 4(b). It can be seen that the flux distribution is distorted due to the eddy current effect of the moving conductor, and the flux pattern is no longer symmetrical with respect to the $y$-axis for all three PM arrays. Also, it can be seen that the flux density in the conductor is much higher for Halbach array (Fig. 2(b)) compared to iron-core PM arrays (Fig. 3(b) and 4(b)). This is more evident in Fig. 5 which shows the $y$-component of the magnetic flux density $B_y$ in the 5 mm air-gap for the different PM arrays when the conductor is present without moving. It can be seen that the maximum magnitude of flux density is about 0.70 T for Halbach array, whereas it is 0.48 T and 0.40 T for horizontally- and vertically-magnetized PM array, re-

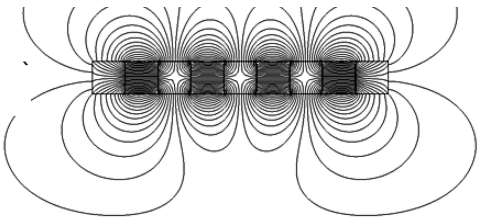

(a)

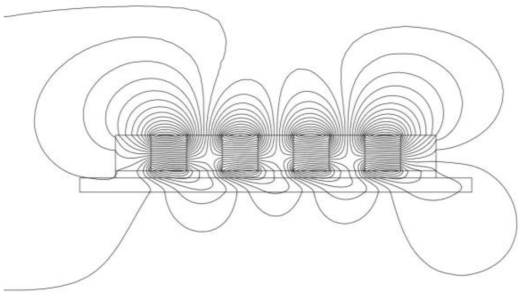

(b)

**Fig. 3.** Magnetic flux distributions of a horizontally-magnetized PM array ⓑ. (a) No conductor. (b) With moving conductor ($v$ = 10 m/s).

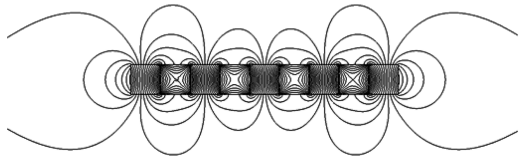

(a)

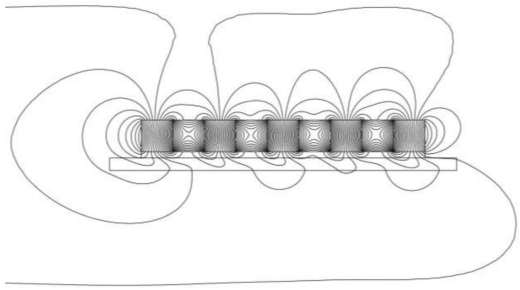

(b)

**Fig. 4.** Magnetic flux distributions of a vertically-magnetized PM array ⓒ. (a) No conductor (b) With moving conductor ($v$ = 10 m/s).

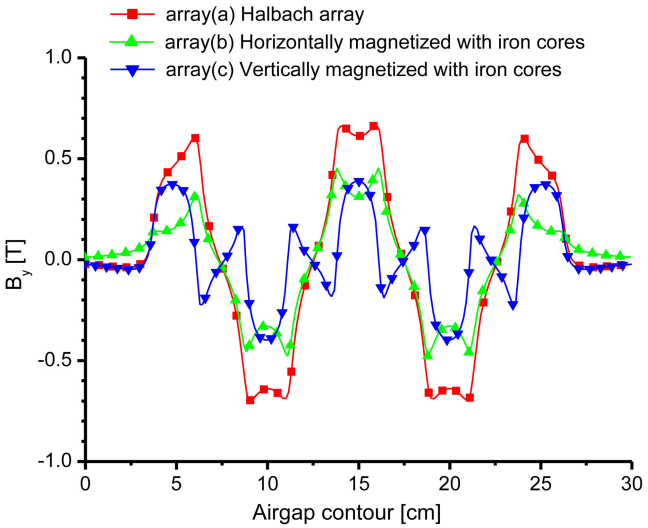


**Fig. 5.** (Color online) Comparison of $y$-component of magnetic flux density ($B_y$) along the cross-section line in the 5 mm air gap for different PM arrays.

spectively.

Fig. 6 shows the braking force characteristics plots with respect to the conductor velocity change. The braking force of Halbach array rises remarkably in proportion to the velocity until it reaches the maximum value of $F_{bf_{max}}$ = 1049 N at $v_m$ = 6 m/s, then it decreases slowly as velocity further increases. The maximum braking force is 294.7 N and 175.1 N for horizontally- and vertically-magnetized PM arrays, respectively. The velocity $v_m$ at which the maximum braking force $F_{bf_{max}}$ occurs is mainly determined by conductivity and thickness of the conductor [9], and this value is similar for all 3 PM arrays.

To summarize this section, after the magnetic field analysis and the braking force calculation of several PM

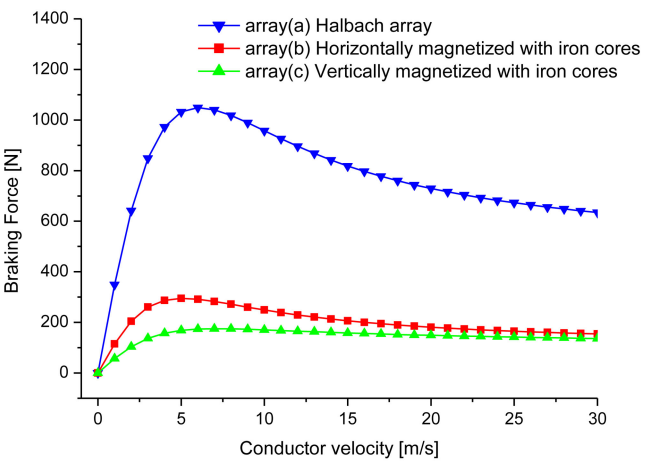


**Fig. 6.** (Color online) Braking force characteristics for different PM arrays.

arrays, it was shown that the Halbach array has several advantages compared to the iron-core PM arrays. Namely, it does not require shielding of magnetic fields on the non-secondary side, and it produces stronger flux density on the secondary conductor side air gap that results in the higher braking force. It should be noted that Halbach array uses more magnets than horizontally- and vertically-magnetized PM arrays, and should have greater braking forces naturally. Thus, we introduce a new performance index in the next section in order to compare the braking performances of different PM arrays.

### 3.2. A new performance index

As we have seen in the previous section, a Halbach array can make up for the disadvantages of the iron-core PM arrays. However, since the Halbach array considered in chapter 3 uses more magnets than iron-core PM arrays, it is difficult to compare the braking forces directly in terms of cost-efficiency, even though the Halbach array has the additional advantage of self-shielding. In other words, when you have more magnets, the magnetic flux density will be naturally higher, but as the volume of the magnet increases, the manufacturing cost will also increase. For this reason, in many of the previous works on eddy current brake design, the volume of the magnet was set to be a constant value [4-7]. However, this constant magnet volume condition imposes severe restrictions on PM array design, and more cost-efficient solutions may not be found. In order to overcome this, a new performance index $p_{br}$ is defined for PM arrays in the eddy current brakes as follows:

$$p_{br} = \frac{|F_{bf_{max}}|}{V_m} \text{ [N/cm}^3\text{]} \tag{8}$$

where $F_{bf_{max}}$ is the maximum braking force in [N] and $V_m$ is the total volume of the magnets in [cm$^3$]. Using this performance index, the 3 PM arrays are compared as shown in Table 2 below.

From above, it can be seen that the Halbach array is much more cost-effective in terms of maximum braking force per magnet volume than iron-core PM arrays, even when the costs of shielding and iron-cores are ignored for

**Table 2.** The maximum braking force $|F_{bf_{max}}|$, performance index $p_{br}$ and total magnet volume $V_m$ for different PM arrays.

| PM array type | $F_{bf_{max}}$ [N] | $p_{br} = \|F_{bf_{max}}\|/V_m$ [N/cm$^3$] | $V_m$ [cm$^3$] |
|---|---|---|---|
| Array ⓐ (Halbach array) | 1049.0 | 3.73 | 281.25 |
| Array ⓑ (Horizontally magnetized) | 294.7 | 2.36 | 125 |
| Array ⓒ (Vertically magnetized) | 175.1 | 1.40 | 125 |

iron-core PM arrays.

## 4. Case Study of Halbach Arrays with a New Performance Index

In this chapter, we perform case study of PM arrays in the eddy current brakes in order to improve the performance index (8). Since a Halbach array was shown to be more cost-efficient than iron-core PM arrays in chapter 3, we chose array a in Fig. 1(a) as an initial model. Then, we change the magnetization directions and dimensions of each magnet block to improve the performance index.

### 4.1. Halbach arrays with different magnetization direction

In this section, we change the length and magnetization directions of each permanent magnet block to improve the braking force per magnet volume. In the proposed structures, the length of each PM block is reduced to 12.5 mm, and the magnetization direction is rotated by $\theta = 45°$ for adjacent PM blocks instead of $\theta = 90°$. Two models are considered here, array ⓓ; a Halbach array with 9 blocks and total length of 112.5 mm (same number of PM blocks as the initial model) and array ⓔ; a Halbach array with 18 blocks and total length of 225 mm (same magnet length as the initial model) (Fig. 7).

Figs. 8 and 9 show comparisons of braking force and braking force per magnet volume versus conductor velocity characteristics. For braking force itself (Fig. 8), new PM array ⓔ with 225 mm total length and 45° magnetization rotation shows the highest maximum braking force value of 1227.0 N, whereas PM array ⓓ with 112.5 mm total length has the lowest maximum braking force value of 563.9 N, lower than 1049 N of the initial model. This is an expected result as the magnet volume in PM array ⓓ is only 50% of those in PM array ⓔ or the initial model. However, in terms of braking force per magnet volume (Fig. 9), array ⓔ has the max value of $p_{br} = 4.36$, followed by array ⓓ with $p_{br} = 4.01$. Initial model has the lowest $p_{br}$ value of 3.73. In other words, both PM arrays ⓓ and ⓔ with 45° magnetization rotation have improved braking force per magnet volume compared to the initial model, with array ⓔ having the higher index. These results are summarized in Table 3 below.

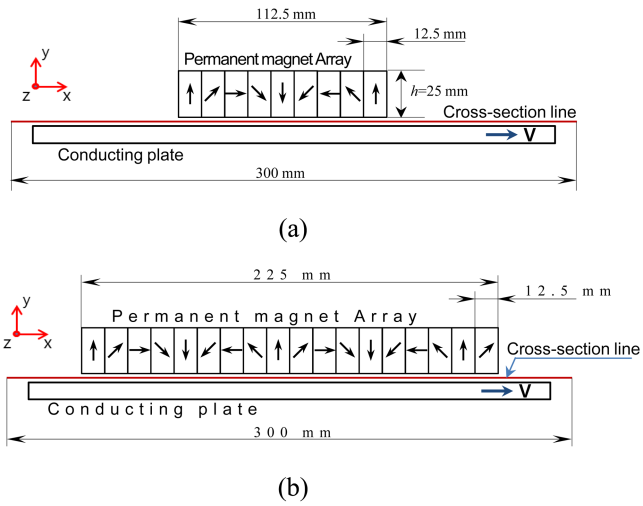


**Fig. 7.** (Color online) Halbach arrays with magnetization direction rotated by $\theta = 45°$ for adjacent blocks. (a) Array ⓓ; 9 blocks and 112.5 mm in total length. (b) Array ⓔ; 18 blocks and 225 mm in total length.

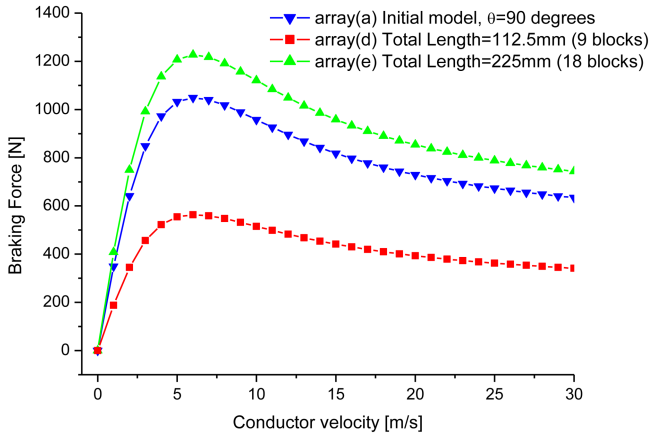


**Fig. 8.** (Color online) Braking force characteristics with different $\theta$ and total magnet length.

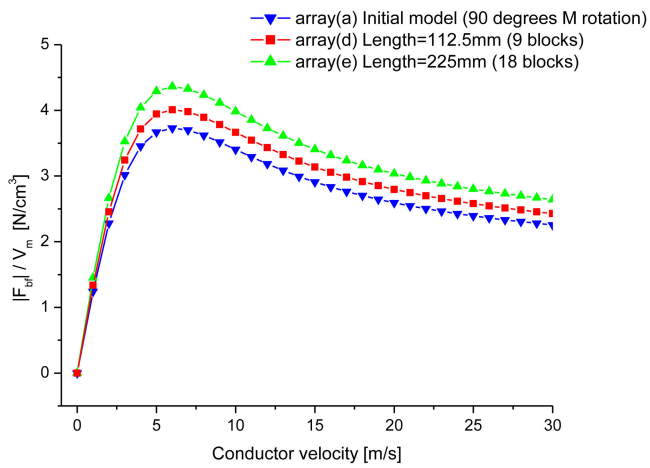


**Fig. 9.** (Color online) Braking force per magnet volume characteristics with different $\theta$ and total magnet length.

### 4.2. Halbach arrays with different heights

Since array e in the previous section has the highest performance index $p_{br}$, we set it as the initial model in this

**Table 3.** The maximum braking force $|F_{bf_{max}}|$, performance index $p_{br}$ and total magnet volume $V_m$ for Halbach arrays with different magnetization direction $\theta$ and total magnet length.

| PM array type | $F_{bf_{max}}$ [N] | $p_{br} = \|F_{bf_{max}}\|/V_m$ [N/cm$^3$] | $V_m$ [cm$^3$] |
|---|---|---|---|
| Array ⓐ (Initial model, $\theta = 90^o$, total magnet length: 225 mm) | 1049.0 | 3.73 | 281.25 |
| Array ⓓ ($\theta = 45^o$, total magnet length: 112.5 mm) | 563.9 | 4.01 | 140.625 |
| Array ⓔ ($\theta = 45^o$, total magnet length: 225 mm) | 1227.0 | 4.36 | 281.25 |

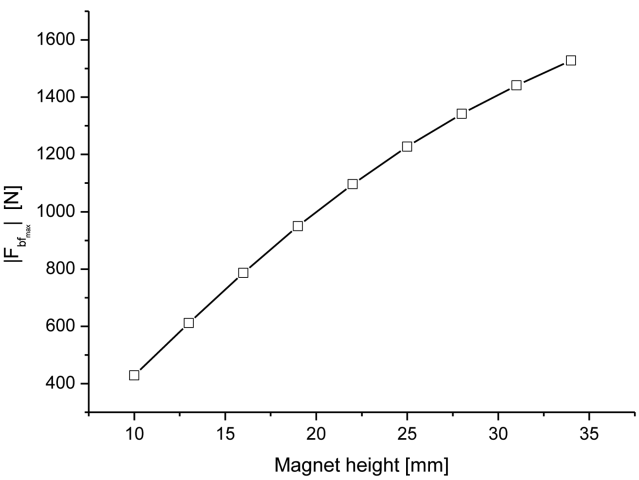


**Fig. 10.** Maximum braking force $|F_{bf_{max}}|$ characteristics for different magnet heights.

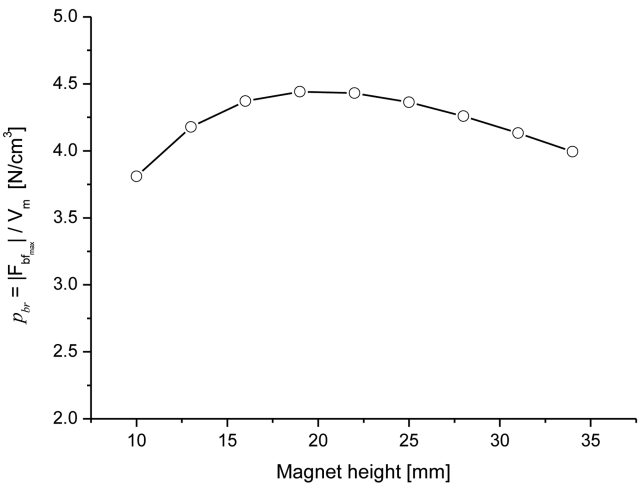


**Fig. 11.** Performance index $p_{br}$ characteristics for different magnet heights.

section. Then, we change the height $h$ of PM blocks from $h = 10$ mm to $h = 34$ mm, increasing it by 3 mm each time, to improve further the braking force and performance index $p_{br}$.

As expected, the maximum braking force itself increases monotonically as the height of the PM array is increased (Fig. 10). However, maximum braking force per magnet volume $p_{br}$ has non-monotonic characteristics, and has the peak at $h = 19$ mm (Fig. 11). For heights between 16 mm $\leq h \leq 25$ mm, $p_{br}$ is greater than 98% of the peak value of 4.44 at $h = 19$ mm, but when $h = 10$ mm or $h = 34$ mm, $p_{br}$ is less than 90% of the peak value. This suggests that when the magnet is too thin ($h = 10$ mm), the magnets are not used efficiently, and when the magnet height exceeds certain limit ($h \geq 34$ mm), increasing the magnet height is not a cost-efficient method to improve the maximum breaking force.

These results for Halbach arrays are also summarized in Table 4. It can be seen that the Halbach arrays with $\theta = 45°$ have significantly higher performance index $p_{br}$ compared to the initial Halbach array with $\theta = 90°$. In particular, PM array with $\theta = 45°$ and $h = 25$ mm has the same magnet volume but 17% higher braking force and $p_{br}$ compared to the initial model. Also, PM array with $\theta = 45°$ and $h = 22$ mm has only 88% of the total magnet volume compared to the initial model, but 4.5% higher

**Table 4.** The maximum braking force $|F_{bf_{max}}|$, performance index $p_{br}$ and total magnet volume $V_m$ for Halbach arrays with different height $h$.

| Halbach array type | $F_{bf_{max}}$ [N] | $p_{br} = \|F_{bf_{max}}\|/V_m$ [N/cm$^3$] | $V_m$ [cm$^3$] |
|---|---|---|---|
| Initial array ($\theta = 90^o$, $h = 25$ mm) | 1049.0 (100%) | 3.73 (100%) | 281.25 (100%) |
| Array ($\theta = 45^o$, $h = 16$ mm) | 786.9 (75.0%) | 4.37 (117.2%) | 180.00 (64%) |
| Array ($\theta = 45^o$, $h = 19$ mm) | 949.6 (90.5%) | 4.44 (119.1%) | 213.75 (76%) |
| Array ($\theta = 45^o$, $h = 22$ mm) | 1096.5 (104.5%) | 4.43 (118.8%) | 247.50 (88%) |
| Array ($\theta = 45^o$, $h = 25$ mm) | 1227.0 (117.0%) | 4.36 (117.0%) | 281.25 (100%) |
| Array ($\theta = 45^o$, $h = 28$ mm) | 1341.6 (127.9%) | 4.26 (114.2%) | 315.00 (112%) |
| Array ($\theta = 45^o$, $h = 31$ mm) | 1441.3 (137.4%) | 4.13 (110.8%) | 348.75 (124%) |

braking force, and 18.8% higher $p_{br}$.

## 5. Conclusion

In this paper, the magnetic field pattern and the braking force characteristics of the eddy current brake systems with different permanent magnet arrays, including Halbach array, were analyzed. Also, in order to compare the cost-efficiency of the magnets used, a new performance index $p_{br}$ was defined as the maximum braking force per total magnet volume. It was shown that the Halbach array had the higher braking force compared to the horizontally- and vertically-magnetized PM arrays with iron-cores. But Halbach array also had higher performance index $p_{br}$ when compared to other arrays. With better braking force characteristics and added advantage of self-shielding of magnetic field, the Halbach array should be the PM array of choice for eddy current brake systems.

To further improve the braking force and $p_{br}$, various Halbach arrays with different magnetization directions $\theta$ and magnet heights $h$ were investigated. It was shown that the Halbach arrays with $\theta = 45°$ (with half-length for each magnet block) have generally higher braking force and $p_{br}$ compared to the initial Halbach array with $\theta = 90°$. The maximum $p_{br}$ occurred when $\theta = 45°$ and $h = 19$ mm.

## Acknowledgment

This work was supported by the Human Resources Development Program (No. 20124010203160) of the Korea Institute of Energy Technology Evaluation and Planning(KETEP) grant funded by the Korea government Ministry of Trade, Industry and Energy.

## References

[1] S. E. Gay, Ph.D. Thesis, Texas A&M University, USA (2005).
[2] P. J. Wang and S. J. Chiueh, IEEE Trans. Magn. **34**, 1237 (1998).
[3] M. Fujita, T. Tokumasu, T. Yamada, T. Hirose, Y. Tanaka, N. Kumagai, and S. Uchida, IEEE Trans. Magn. **34**, 3548 (1998).
[4] J.-S. Choi and J. Yoo, IEEE Trans. Magn. **44**, 2361 (2008).
[5] S.-M. Jang, S.-S. Jeong, and S.-D. Cha, IEEE Trans. Magn. **37**, 2627 (2001).
[6] H.-R. Cha, H.-W. Cho, and S.-H. Lee, J. Electr. Eng. Technol. **3**, 379 (2008).
[7] A. Canova and B. Vusini, IEEE Trans. Ind. Appl. **39**, 725 (2003).
[8] COMSOL Inc.(<www.comsol.com>).
[9] J. D. Edwards, B. V. Jayawant, W. R. C. Dawson, and D. T. Wright, IEE Proc.-Electr. Power Appl. **146**, 627 (1999).
[10] C. Ham, W. Ko, and Q. Han, J. Appl. Phys. **99**, 08P510 (2006).